THE ASTROPHYSICAL JOURNAL, 338:171–177, 1989 March 1

84 GIGAHERTZ OBSERVATIONS OF FIVE CRAB-LIKE SUPERNOVA REMNANTS

C. J. SALTER
Instituto de Radioastronomia Milimetrica, Spain
S. P. REYNOLDS
North Carolina State University
AND
D. E. HOGG, J. M. PAYNE, AND P. J. RHODES
National Radio Astronomy Observatory
Received 1988 June 6; accepted 1988 August 13

ABSTRACT

We have observed five Crab-like supernova remnants with the NRAO[1] 12 m telescope at 84.2 GHz. Four were detected. In three of these four cases, the observed flux falls below the extrapolation from centimeter wavelengths, although with varying degrees of significance. Spectral steepening may result from an intrinsic break in the particle spectrum injected by the pulsar presumed to power each object, or it may reflect evolutionary changes. If our three lower than expected flux densities were to be due to steepening caused by evolutionary effects, severe constraints can be put on the characteristics of the objects showing spectral steepening: all must be less than 2000 yr old, and the supernovae in which they were born must all have had very unusual properties. Further observations in the frequency range between 30 and 300 GHz are essential to clarify the nature of the possible steepening.

Subject headings: nebulae: supernova remnants — radio sources: identifications

I. INTRODUCTION

The evolution of the emitted synchrotron spectrum of a pulsar-driven, expanding nebula has been studied in detail by Pacini and Salvati (1973), Reynolds and Chevalier (1984), and Reynolds and Chanan (1984). The observed class of filled-center supernova remnants (Crab-like SNRs or plerions), the subject of the review by Weiler (1985), is believed to comprise objects of this type. Reynolds and Chanan demonstrated that the characteristic continuum spectrum should consist of either two or three frequency intervals, depending on evolutionary phase, having different spectral indices and separated by distinct break frequencies that change with time. They identify the radio region with the lowest frequency regime, where the spectral index is expected to mirror the energy dependence of the relativistic electrons injected into the nebula by the supposed central pulsar.

Of the claimed Crab-like SNRs and Crab-like components within shell-type SNRs (Weiler 1985), only G27.8+0.6 has been found to show a spectral break below 10 GHz (Reich, Fürst, and Sofue 1984). However, recent observations by Morsi and Reich (1987) reveal another object, G74.9+1.2, to have a break between 11 and 32 GHz. For the Crab Nebula itself, a break has been localized by observations in the millimeter/submillimeter region (Marsden *et al.* 1984), where a turnover is found at $\sim 10^4$ GHz. Clearly, such breaks are important indicators of physical conditions within the nebula and it is of interest to extend observations of all Crab-like SNRs into the millimeter and submillimeter bands. For a two-part spectrum, characteristic of relatively young remnants (age $t \lesssim 1000$ yr), the break results from synchrotron losses and its location gives information on the magnetic field strength. In older remnants with three-part spectra, the spectral index of the middle segment contains dynamical information, while the indices of the other two segments are related to the energy spectrum of the relativistic electrons at injection (Reynolds and Chanan 1984).

In the present study, we have made flux density measurements at 3.6 mm wavelength to extend the frequency coverage for three Crab-like remnants and two Crab-like components within remnants whose larger scale morphologies show shell-type structure. All five objects show the flat, polarized nonthermal radio spectra and associated X-ray emission characteristic of this class.

II. OBSERVATIONS AND ANALYSIS

The observations were made on 1985 December 26–28 with the NRAO 12 m millimeter-wave telescope at an effective frequency of 84.2 GHz. The standard, dual-channel, 3 mm Schottky mixer receiver was used with a double-sideband noise temperature of ~ 140 K and a bandwidth of 600 MHz per channel. Receiver gain was calibrated regularly via a noise source located at the center of the telescope subreflector. All observations were made in the beam-switched mode using the nutating subreflector to produce two beams separated by 4′.

Telescope pointing was determined on strong sources and checked frequently throughout the observations. "Skytips" were taken at ~ 90 minute intervals to measure the atmospheric extinction. Maps of the telescope beam gave an HPBW of $76'' \times 70''$. The flux density and brightness temperature scales of the observations were calibrated via measurements of the planets Mars, Saturn, and Jupiter. Planetary disk temperatures were taken from Ulich (1981). The internal consistency among the three planets was $\pm 4\%$, and it is believed that the flux density and temperature scales are correct to $\sim 5\%$. In addition to the planets, three strong sources were used for pointing; they are listed in Table 1, with the peak flux densities we derived from these observations. For DR 21 an integrated flux density of 16.1 ± 1.1 Jy results after applying a correction

[1] The National Radio Astronomy Observatory is operated by Associated Universities, Inc., under contract with the National Science Foundation.

TABLE 1

SOURCES USED FOR POINTING DETERMINATIONS

Source	Peak Flux Density
DR 21	14.9 ± 1.0 Jy
3C 84	35.0 ± 2.5 Jy
3C 273	10.1 ± 0.7 Jy

for beam-broadening equivalent to that used by Ulich (1981). This compares with the same author's value of 17.0 ± 0.5 Jy. H. Steppe (personal communication) measured flux densities at 90 GHz of 35.6 ± 2.3 Jy for 3C 84 and 9.8 ± 0.5 Jy for 3C 273 in early 1986 January with the IRAM 30 m telescope.

The five Crab-like objects observed were G21.5−0.9, the flat-spectrum component in G29.7−0.3, the central core of CTB 80 (G68.9+2.8), G74.9+1.2 (CTB 87), and 3C 58 (G130.7+3.1). They are listed in Table 2. The best available radio positions were taken from the published literature. As G21.5−0.9, the core of G29.7−0.3, and the core of CTB 80 are all smaller than, or of similar size to, the telescope beam, their flux densities were determined via ON-ON measurements. For this, the source position was alternately placed in the positive and negative beams of the dual-beam pattern, the intensity difference being taken to determine the peak flux density. The integration times achieved are given in Table 2. Five-point maps were made of G21.5−0.9, the brightest and most extended of these three, in order to estimate directly the associated beam broadening.

Fully sampled maps of size 18′ × 12′ were made for both G74.9+1.2 and 3C 58. Integration times per 30″ × 30″ pixel were 10 and 25 s, respectively, for the sources.

The data were analyzed on the IRAM (Granada) VAX 11/780 computer using the NRAO CONDAR package, with the NOD2 map-processing library (Haslam 1974) running under the control of CONDAR. The dual-beam maps of G74.9+1.2 and 3C 58 were processed via the algorithm of Emerson, Klein, and Haslam (1979), which permits reconstruction of the image as if observed with the equivalent single beam. Maps of point sources were also observed and processed through the same algorithm to provide calibration standards. A full-beam solid angle of 1.33×10^{-7} sr was derived for an area of 4′ × 4′. This gives a point-source flux density to effective full-beam brightness temperature ratio of 29 Jy K^{-1}. At full resolution the final maps had rms noises of 7.2 mK for G74.9+1.2 and 4.2 mK for 3C 58.

III. RESULTS

The peak brightnesses derived from the ON-ON measurements for G21.5−0.9, G29.7−0.3 and CTB 80 are given in Table 2. From the five-point maps of G21.5−0.9, a deconvolved effective Gaussian FWHM of 50″ ± 10″ was obtained. This width was used in deriving the integrated flux density included in Table 2.

The contour map of G74.9+1.2 showed no significant structure greater than the noise level at full resolution. The map of 3C 58, smoothed to a resolution of 90″ to improve the signal-to-noise ratio, is shown in Fig. 1. The contour interval is 5 mK of full-beam brightness temperature. From this map, the 84.2 GHz integrated flux density of this source is found to be 15.0±2.0 Jy.

a) Individual Sources

i) *G21.5−0.9*

The measured FWHM of 50″ ± 10″ for G21.5−0.9 is consistent with previous estimates (49″ × 54″ by Wilson and Weiler 1976; 51″.5 × 35″ by Becker and Kundu 1976). In the radio region, Wilson and Weiler found a constant flux density of ~6.4 Jy to apply between 80 MHz and 10.7 GHz. Morsi and Reich (1987) report 5.6 ± 0.3 Jy at 32 GHz, a difference they do not find significant. Our integrated 84.2 GHz flux density of 3.9 ± 0.7 Jy is significantly below the lower frequency fluxes (Fig. 2*a*). It implies a spectral index α ($S_\nu \propto \nu^\alpha$) of −0.37 ± 0.19 between 32 and 84 GHz. Perhaps the slightly lower flux density obtained by Morsi and Reich, regarded by them as insignificantly different from the centimeter-wave value, in fact represents the beginning of the downturn that we observe at 84 GHz. This downturn has been confirmed by recent observations at 90 and 142 GHz (also shown in Fig. 2*a*) with the IRAM 30 m telescope (Emerson *et al.* 1989). It is interesting to note that a downturn below 80 GHz is barely consistent with the extrapolation all the way back from X-ray wavelengths of the X-ray spectrum observed by Davelaar, Smith, and Becker (1986).

ii) *G29.7−0.3*

The semicircular, steep-spectrum remnant G29.7−0.3 contains the amorphous Crab-like component which we have observed. If we assume that the equivalent FWHM measured for this component in the radio of 26″ × 17″ (Hunt *et al.* 1989) also applies at 84 GHz, then our peak brightness from Table 2 would correspond to an integrated value of 159 ± 18 mJy. Becker and Helfand (1984) measured a flux density of 275 mJy at wavelengths of 2, 6, and 20 cm, and at first sight these data would appear to indicate a spectral steepening between 15 and 84 GHz ($\alpha \cong -0.3$). However, they quoted no errors, making a quantitative statement difficult. However, Hunt *et al.* (1989) obtain flux densities of 348, 247, and 172 mJy at 1.4, 4.9, and 15.0 GHz, respectively, for this component, which imply a straight spectrum having $\alpha = -0.20 \pm 0.05$ over the frequency range 1.4–84 GHz (Fig. 2*b*). It is interesting that Becker and Kundu (1976) also derived a mildly negative spectral index of −0.27 ± 0.15 for this component. Further observations with a

TABLE 2

OBSERVED SOURCES

Source	Integration Time	Peak Brightness (mJy beam^{-1})	Integrated Flux Density (Jy)
G21.5−0.9	20 minutes	2675 ± 200	3.94 ± 0.70
G29.7−0.3 (core)	132 minutes	147 ± 16	...
CTB 80 (G68.9+2.8)	60 minutes	254 ± 26	...
G74.9+1.2 (CTB 87)	10 s pixel^{-1}	<600	...
3C 58 (G130.7+3.1)	25 s pixel^{-1}	...	15.0 ± 2.0

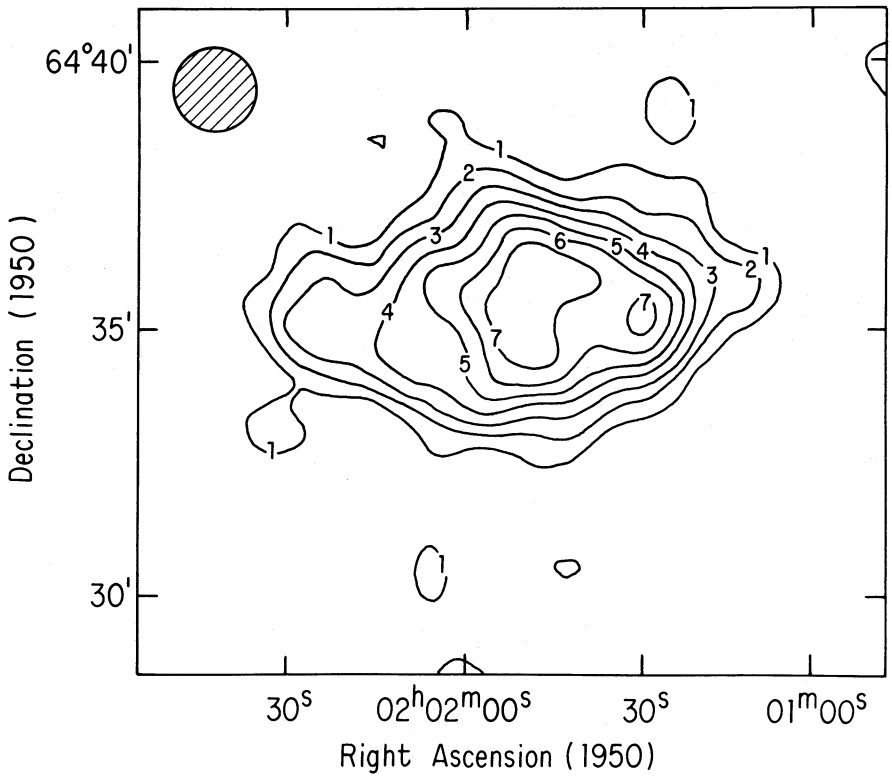

FIG. 1.—The 84.2 GHz map of G130.7+3.1 (3C 58). The resolution is 90″, as shown in the top left-hand corner of the map. The contour interval is 5 mK of full-beam brightness temperature.

wider frequency coverage are needed to clarify the situation fully. However, we conclude that the total set of spectral data for the core of G29.7−0.3 shown in Figure 2*b* provides no evidence for a spectral break below 84 GHz.

iii) *CTB 80*

Perhaps the most enigmatic of extended Galactic nonthermal sources, the nebula CTB 80 contains the small diameter, flat spectrum core observed here (Angerhofer *et al.* 1981; Velusamy and Kundu 1983; Strom 1987), as well as the newly discovered 39.5 ms pulsar (Kulkarni *et al.* 1988; Fruchter *et al.* 1988). Despite the large-scale limb-brightened shell morphology, the central component has a flat spectrum and associated X-ray emission and has frequently been classified as a Crab-like object. Angerhofer *et al.* found a constant flux density of 500 mJy (no errors quoted) to apply at all wavelengths between 2.8 and 49 cm, while Sofue *et al.* (1983) measured a value of 440 ± 100 mJy at a frequency of 10.2 GHz. We adopt a FWHM of 30″ ± 10″ for the source giving an integrated flux density at 84 GHz of 297 ± 45 mJy. Although an element of steepening may be present between 10 and 84 GHz, a spectral index of −0.1 throughout the whole frequency range would differ from none of the above measurements by more than 15% (Fig. 2*c*). With no errors for the Angerhofer *et al.* points, a more quantitative statement cannot be made.

iv) *G74.9+1.2*

Morsi and Reich (1987) measured a 32 GHz flux density for this object of 1.47 ± 0.19 Jy, considerably below the extrapolation from lower frequencies using the spectral index of −0.24±0.15 found by Weiler and Shaver (1978). If characteristic of the millimeter-wave region, their derived two-point spectral index of −1.1 between 11 and 32 GHz implies a flux density of 0.51 Jy at 84 GHz. Our full-resolution map shows no structure above noise. While comparison of a version of our data smoothed to 4′.4 resolution with the high-sensitivity 2.7 GHz observations of Geldzahler, Pauls, and Salter (1980) suggests that spectral curvature is probably present between 2.7 and 84 GHz, we can add nothing quantitative to the conclusions of Morsi and Reich. A millimeter-wave map of considerably higher sensitivity is required before definite conclusions can be drawn on the detailed spectral shape of this source above 30 GHz.

v) *3C 58*

Using the present 84.2 GHz flux density, that of Morsi and Reich (1987) at 32 GHz, and values from Green (1986), the integrated spectrum of 3C 58 is shown in Figure 2*d*. The line plotted on Figure 2*d* is the best-fit straight-line spectrum; the derived spectral index is −0.11+0.01 including our 84 GHz point (−0.10±0.01 without it). While the 84 GHz point lies somewhat below the line and could indicate a steepening setting in near or above 32 GHz, it is not grossly inconsistent with a continuation of the straight radio spectrum. A flux density at 1 mm wavelength would be crucial for determining the actual spectral shape in the millimeter region.

The full-resolution map was smoothed to the 72″ × 80″ resolution of the 151 MHz study of Green (1986) and the two maps compared to give the distribution of spectral index over the source for a frequency ratio of 550:1. Above the 5 σ level at 84 GHz (20 mK) the mean spectral index is −0.14, exactly equal to the value derived from the integrated fluxes at the two frequencies. The standard deviation for the spectral index distribution is 0.045. There are no significant indications for variations of the index across the remnant; a slight preference

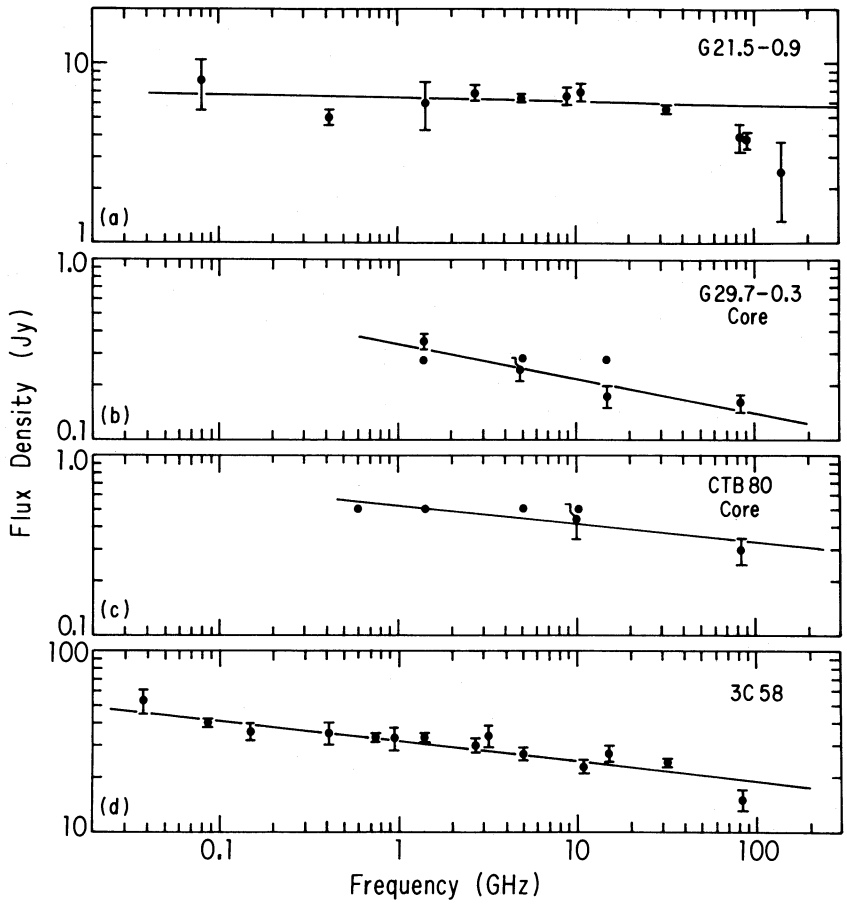

FIG. 2.—The continuum spectra of Crab-like SNRs. In addition to the present 84.2 GHz measurements, data are from the literature. (*a*) The continuum spectrum of G21.5−0.9. The 84.2 GHz result is from this paper. Other points are from Wilson and Weiler (1976), Becker and Kundu (1975), Morsi and Reich (1987), and Emerson *et al.* (1989). The plotted line gives a spectral index of $\alpha = -0.02$. (*b*) The continuum spectrum of the central component of G29.7−0.3. The 84.2 GHz result is from this paper. Other points are from Becker and Helfand (1984, quoted without errors) and Hunt *et al.* (1989). The plotted line gives a spectral index of $\alpha = -0.2$. (*c*) The continuum spectrum of the core of G68.9+2.8 (CTB 80). The 84.2 GHz result is from this paper. Other points are from Angerhofer *et al.* (1981; quoted without errors) and Sofue *et al.* (1983). The plotted line gives a spectral index of $\alpha = -0.1$. (*d*) The continuum spectrum of G130.7+3.1 (3C 58). The 84.2 GHz result is from this paper. Other points are from Green (1986) and Morsi and Reich (1987). The plotted line gives a spectral index of $\alpha = -0.11$.

for lower indices to occur near the edge of the object is felt likely to be due to residual tracking and pointing errors of the 12 m telescope.

IV. DISCUSSION

Despite excellent agreement between the measured 84 GHz flux densities of standard radio sources observed during the experiment and the other available estimates of their flux densities (see § II), the measurements for G21.5−0.9, CTB 80, and 3C 58 lie tantalizingly below those estimated from their centimeter-wave spectra. The data of Morsi and Reich (1987) establish that in addition there is spectral steepening for G74.9±1.2. Thus for four of the five Crab-like objects studied at millimeter wavelengths there is the possibility of a steepening of the spectrum at short wavelengths. Indeed, the trend is sufficiently intriguing that the measurement of integrated flux densities at 1 mm wavelength, especially for G29.7−0.3, G68.9+2.8, and G74.9+1.2, assumes great importance.

To put our subsequent discussion in perspective, we shall summarize the quantitative results.

1. Our data were inconclusive on G74.9+1.2, but Morsi and Reich (1987) found their 32 GHz flux to fall $\sim 11\ \sigma$ below the lower frequency extrapolation.

2. We find the 84 GHz flux density of the core of G29.7−0.3 to be consistent with the spectrum derived from the centimeter-wavelength data of Hunt *et al.* (1989).

3. We find the 84 GHz flux densities of G21.5−0.9, 3C 58 and CTB 80 to lie $\sim 3.5\ \sigma$, $3\ \sigma$, and $4.5\ \sigma$, respectively, below the lower frequency extrapolations. Furthermore, a break in the spectrum of G21.5−0.9 seems confirmed by the new IRAM 30 m observations (§ III*a*[i]).

Morsi and Reich (1987) claim unambiguous evidence for a steepening of the spectrum of G74.9+1.2. Our data on G21.5−0.9, coupled with Morsi and Reich's slightly low 32 GHz point and the new IRAM results, lead us to believe that, here too, the presence of steepening is secure. As detailed in the previous section, the results for 3C 58 and CTB 80, on the edge of significance, cannot be judged to be conclusive evidence for steepening. However, we feel that the data are sufficiently suggestive that the possibility that all four objects have spectra that steepen between 30 and 84 GHz must be taken seriously.

Various explanations can be advanced for the observed flux densities. The most conservative suggestion, that the fluxes for

3C 58 and CTB 80 are consistent with the lower frequency spectra, lets us conclude nothing about these objects except that they are different from G21.5−0.9 and G74.9+1.2, two otherwise similar Crab-like objects that do show spectral breaks. We shall discuss briefly the consequences of assuming that the deficits are real, that is that the radio spectra of these objects become steeper somewhere in the interval between 10 or 30 GHz and our frequency of 84 GHz. Since this seems to be the case for two of the four, and certainly possible for the other two, we shall discuss all four together. Should the breaks in 3C 58 and CTB 80 be confirmed by future observations above 100 GHz, the conclusions that we reach below will need to be considered in interpreting the situation.

The simplest explanation for a steepening is that it is intrinsic; that is, the pulsars presumed to power each object could simply inject electrons with an energy spectrum that steepens at the appropriate energy, due to some effect in the unknown acceleration process. Rough estimates of the equipartition fields B_{eq} in each object using standard formulae (Pacholczyk 1970) give $\sim 10^{-4}$ G in each case, if one roughly approximates each object's spectrum as that of the centimeter-wavelength spectral index unbroken to 10^{11} Hz. (If the spectra all cut off completely above 30 GHz, the integrated radio luminosity L_r would be lower by less than a factor of 3, and $B_{eq} \propto L_r^{2/7}$ would be only 40% lower.) Then electrons radiating at 30 GHz have energies of ~ 10 GeV in all cases. A break at this energy may be common for some reason in spectra of electrons accelerated by pulsars. It cannot be universal, however; the Crab Nebula's spectrum does not show such a break.

For G74.9+1.2, the flux densities measured at 32 GHz by Morsi and Reich (1987) and at 10.7 GHz by Green, Baker, and Whiteoak (unpublished; quoted in Weiler and Shaver 1978) give a steepening above 10 GHz of at least 0.8 in the spectral index. This is too large to be explained by any straightforward evolutionary effect and, if confirmed, implies some intrinsic steepening mechanism here too. However, a steepening by only 0.5, such as could be produced by the mechanisms described below, is within the 1 σ limits on the measurements at each frequency. We also note that Duin *et al.* (1975) obtained a lower flux density at 10.6 GHz than that of Green, Baker, and Whiteoak, and stress the importance of an improved measurement near this frequency.

Evolutionary effects will steepen an initially flatter injected energy spectrum of particles (Pacini and Salvati 1973; Reynolds and Chevalier 1984; Reynolds and Chanan 1984). At times less than the pulsar's slowdown time scale τ (of order 1000 yr for a pulsar born rotating with a period of 10 ms and a magnetic field of 10^{12} G), the electron spectrum breaks due to synchrotron losses at an energy that rises with time. Above the break the electron spectrum is one power steeper, as in the homogeneous case, so the photon spectrum steepens by one-half power. At times longer than τ, a second break energy appears below the first, and moves with time to lower frequencies. However, the amount of steepening in the electron energy spectrum there is small, implying less than 0.2 steepening in the photon spectrum. After considerably longer times (of order 10,000 yr), a reverse shock moves back in; the evolution is quite different thereafter (Reynolds and Chevalier 1984).

If we take our observations at face value, they imply a steepening too great to be due to anything but synchrotron losses or post–reverse-shock evolution. The latter possibility can be immediately dismissed; applying the results of Reynolds and Chevalier (1984), one finds that the steep break occurs at much higher frequencies than 100 GHz at all times. The synchrotron-loss interpretation is barely consistent with both our data and that of Morsi and Reich (1987). Then the evolutionary model of Reynolds and Chevalier (1984) implies that all these objects have ages less than their pulsars' slowing-down times τ, a remarkable conclusion. Assuming the radio spectrum steepens abruptly by 0.5 at the break frequency ν_b, we find $\nu_b \cong 30$ GHz for G21.5−0.9 and CTB 80, and $\nu_b \cong 40$ GHz for 3C 58. For G74.9+1.2, a steepening by 0.5 can be accommodated by the data, as mentioned above; this would imply $\nu_b \cong 6$ GHz.

For G21.5−0.9 and 3C 58, a spectrum steeper by 0.5 extrapolated from 84 GHz to the X-ray region is marginally consistent with X-ray data. Observations of the X-ray spectra of these objects by Davelaar, Smith, and Becker (1986) imply mean spectral indices between 84 GHz and 4 keV of −0.85 and −1.0, respectively, whereas the spectral indices in X-rays alone are -0.77 ± 0.12 and -1.30 ± 0.26, respectively. However, even if the X-ray spectral indices are shown to be inconsistent with the millimeter-to-X-ray extrapolations, this would be only weak evidence against the synchrotron-loss interpretation, since the Crab Nebula has more complicated spectral structure intervening between radio and X-rays, and these objects should as well (Reynolds and Chanan 1984).

Detailed models have been calculated in the Reynolds-Chevalier scheme for G21.5−0.9, CTB 80, and 3C 58, with the results shown in Table 3. Values for the Crab Nebula are included for comparison. Since our data do not cast light on the spectrum of G74.9+1.2, we have not modeled it. However, the very low implied break frequency, along with the remnant's large size and low surface brightness, would demand parameter values even more extreme than those of Table 3. The

TABLE 3

EVOLUTIONARY MODEL PARAMETERS

Source	Distance (kpc)	Age (yr)	L_0 (10^{40} ergs s^{-1})	M_c ($M_\odot$)	v_1 (km s^{-1})	τ (yr)	P_0 (ms)	P(now) (ms)
G21.5−0.9	4.8	820	2	7.2	300	1000	6.4	9.4
CTB 80	2	1600	0.0004[a]	5	130	140,000[a]	40[a]	40[a]
3C 58	2.6	807[a]	34	43	4000	900	1	2.6
Crab Nebula	2	934[a]	0.85[b]	2[b]	300[b]	744	19	33[a]

NOTE.—L_0, M_c, and v_1 are the initial pulsar luminosity, the mass of ejecta (either the progenitor mantle, moving relatively slowly, or the entire progenitor mass, with greater velocity [homogeneous model]), and the velocity of the outer edge of the ejecta (core or total mass). The model for 3C 58 is homogeneous.

[a] Observed value.

[b] Values from Reynolds and Chevalier 1984.

young age for CTB 80 does not conflict with the observed spin-down age $t_c \equiv P/2\dot{P} \sim 10^5$ yr (Fruchter *et al.* 1988) since for $t < \tau$ as assumed, $t_c \cong t + \tau \cong \tau$.

The Reynolds-Chevalier models detailed in Table 3 all assume pulsar braking indices of 2.5, though the results are very insensitive to this value. The important parameters are then the core mass M_c, its outer velocity v_1, and the pulsar initial spindown power L_0, with the additional stipulation that the age be less than τ. A model is then almost completely specified by an observed v_b, mean radius R, and another observable such as age t. The models for 3C 58 (age known) and CTB 80 (current pulsar luminosity known; Fruchter *et al.* 1988) are then well constrained. For G21.5−0.9, only two of these observables are known, so the solution is not unique; but allowable values of the three parameters are related, and the quoted values represent attempts to keep all three in sensible ranges. (The Crab Nebula model is very well constrained since the age, current pulsar luminosity, and current braking index are all known; see Reynolds and Chevalier 1984 for details.)

The new models require large values for core mass or (for 3C 58) total ejected mass. Further, the pulsars in 3C 58 and G21.5−0.9 must be quite powerful. This arises because the remnants are all fairly large, yet they must be young in order that the magnetic field strength be large enough to compel a break frequency as low as is observed. Even so, the inferred model parameters for G21.5−0.9 and CTB 80 are not totally unreasonable. However, for CTB 80, recent observations (Fesen, Shull, and Saken 1988) seem consistent with a very large true age for the object as suggested by the large spin-down age, again casting doubt on the evolutionary explanation for any spectral break. As well, for 3C 58, the ejected mass is much greater than derived in the usual models of supernovae. In addition, the initial pulsar luminosity would have been extraordinarily high. We conclude that such properties are unlikely and that if spectral breaks are present in the region of 30 GHz for any of the sources considered, these are more likely due to intrinsic structure in the energy spectrum of the relativistic electrons generated by the pulsar than to this evolutionary picture.

We note in passing that while the evolutionary models described in Table 3 imply that three new fast pulsars have been born in less than 2000 yr, this result is not in conflict with pulsar statistics. If those evolutionary models are correct, the three modeled objects with the Crab Nebula would represent four plerions born in the last 2000 yr containing pulsars with initial periods below 40 ms. Objects this young would need a plerion birth rate greater than ~ 1 per 500 yr. This is to be compared with the pulsar birth rate derived by Lyne, Manchester, and Taylor (1985) which can be written as 1 per $240(\Delta\Omega/4\pi)$ yr, where $\Delta\Omega$ is the solid angle of sky swept by pulsar beams. If beaming factors are in the range 0.2–0.5 then 4–10 times more young plerions than required can be accommodated by the Lyne, Manchester, and Taylor pulsar birth rate. In this picture, young Crab-like objects are normally quite unspectacular. The Crab Nebula would then owe its unique brightness to a combination of unusually low M_c and fairly low v_1, rather than a special pulsar.

V. SUMMARY

We have observed five Crab-like supernova remnants at 84 GHz, and find that in three cases, the observed flux density is lower than that expected on the basis of an extrapolation of the spectrum from lower frequencies. In one case, we find just the flux density expected from the lower frequency extrapolation. For the remaining object, our results are inconclusive, but Morsi and Reich (1987) find a lower than expected flux density at 32 GHz. If these deficits are real, they could be due to intrinsic structure in the energy spectrum of relativistic electrons generated by the pulsars or to evolutionary effects. In the latter case, the implied break is due to synchrotron losses. Such an interpretation demands that all the objects be less than 2000 yr old and powered by rapid pulsars, two of which are predicted to have periods shorter than 10 ms. However, the models require somewhat unreasonable parameters; for instance, the progenitor mass of 3C 58 must have been greater than ~ 45 $M_\odot$. Should spectral steepening consistent with our 84 GHz measurements be confirmed for any of the plerions considered, we believe that intrinsic spectral structure is a more plausible explanation for such steepening.

A minor consequence of these results is that calculations of the radio luminosity L_r of Crab-like supernova remnants, frequently obtained by integrating the presumed unbroken centimeter-wave spectrum between 10^7 and 10^{11} Hz, may frequently overestimate the true radio luminosity in this frequency range by factors of a few. We suggest caution in the use of such extrapolations for Crab-like remnants.

Clearly, further investigation of the possible spectral steepening at millimeter wavelengths is crucial to progress. Additional observations between 30 and 90 GHz could localize any steepening. Observations with small telescopes in the 1 mm band, where practical, might provide the best tests, although the substantial angular size and low surface brightness of these objects make that a difficult experiment.

Finally, we note that, where sensitivity permits, detailed mapping at millimeter wavelengths gives both increased information and more accurate integrated flux densities compared with ON-ON measurements. Such mapping should be possible for sources in the present sample of remnants at both 1 and 3 mm with the new generation of millimeter-wave receivers and telescopes.

The authors would like to thank the staff of the 12 m telescope for their assistance during the observations. Betty Stobie is especially thanked for her invaluable assistance in bringing up CONDAR at a transatlantic distance. S. P. R. thanks Research Corporation for support.

REFERENCES

Angerhofer, P. E., Strom, R. G., Velusamy, T., and Kundu, M. R. 1981, *Astr. Ap.*, **94**, 313.
Becker, R. H., and Helfand, D. J. 1984, *Ap. J.*, **283**, 154.
Becker, R. H., and Kundu, M. R. 1975, *A.J.*, **80**, 679.
———. 1976, *Ap. J.*, **204**, 427.
Davelaar, J., Smith, A., and Becker, R. H. 1986, *Ap. J. (Letters)*, **300**, L59.
Duin, R. M., Israel, F. P., Dickel, J. R., and Seaquist, E. R. 1975, *Astr. Ap.*, **38**, 461.
Emerson, D. T., Klein, U., and Haslam, C. G. T. 1979, *Astr. Ap.*, **76**, 92.
Emerson, D. T., Salter, C. J., Steppe, H., and Thum, C. 1989, in preparation.
Fesen, R. A., Shull, J. M., and Saken, J. M. 1988, *Nature*, **334**, 229.
Fruchter, A. S., Taylor, J. H., Backer, D. C., Clifton, T. R., Foster, R. S., and Wolszczan, A. 1988, *Nature*, **331**, 53.
Geldzahler, B. J., Pauls, T., and Salter, C. J. 1980, *Astr. Ap.*, **84**, 237.
Green, D. A. 1986, *M.N.R.A.S.*, **218**, 533.
Haslam, C. G. T. 1974, *Astr. Ap. Suppl.*, **15**, 333.
Hunt, G. C., Patnaik, A. R., Salter, C. J., and Shaver, P. A. 1989, in preparation.
Kulkarni, S., Clifton, T. R., Backer, D. C., Foster, R. S., Fruchter, A. S., and Taylor, J. H. 1988, *Nature*, **331**, 50.
Lyne, A. G., Manchester, R. N., and Taylor, J. H., 1985, *M.N.R.A.S.*, **213**, 613.

Marsden, P. L., Gillett, F. C., Jennings, R. E., Emerson, J. P., De Jong, T., and Olnon, F. M. 1984, *Ap. J. (Letters)*, **278**, L29.
Morsi, H. W., and Reich, W. 1987, *Astr. Ap. Suppl.*, **69**, 533.
Pacholczyk, A. G. 1970, *Radio Astrophysics* (San Francisco: Freeman).
Pacini, F., and Salvati, M. 1973, *Ap. J.*, **186**, 249.
Reich, W., Fürst, E., and Sofue, Y. 1984, *Astr. Ap.*, **133**, L4.
Reynolds, S. P., and Chanan, G. A. 1984, *Ap. J.*, **281**, 673.
Reynolds, S. P., and Chevalier, R. A. 1984, *Ap. J.*, **278**, 630.
Sofue, Y., Takahara, F., Hirabayashi, H., Inoue, M., and Nakai, N. 1983, *Pub. Astr. Soc. Japan*, **35**, 437.
Strom, R. G. 1987, *Ap. J. (Letters)*, **319**, L103.
Ulich, B. L. 1981, *A.J.*, **86**, 1619.
Velusamy, T., and Kundu, M. R. 1983, *J. Ap. Astr.*, **4**, 253.
Weiler, K. W. 1985, in *The Crab Nebula and Related Supernova Remnants*, ed. M. C. Kafatos and R. B. C. Henry (Cambridge; Cambridge University Press), p. 227.
Weiler, K. W., and Shaver, P. A. 1978, *Astr. Ap.*, **70**, 389.
Wilson, A. S., and Weiler, K. W. 1976, *Astr. Ap.*, **53**, 89.

DAVID E. HOGG: National Radio Astronomy Observatory, Edgemont Road, Charlottesville, VA 22903-1797

J. M. PAYNE and P. J. RHODES: National Radio Astronomy Observatory, 949 North Cherry Avenue, Campus Building 65, Tucson, AZ 87521-0655

STEPHEN P. REYNOLDS: Department of Physics, North Carolina State University, Box 8202, Raleigh, NC 27695-8202

C. J. SALTER: Nuffield Radio Astronomy Laboratories, Jodrell Bank, Macclesfield, Cheshire SK11 9DL, England, UK